

Non-equilibrium evolution of window overlaps in spin glasses

Markus Manssen,¹ Alexander K. Hartmann,¹ and A. P. Young²

¹*Institute of Physics, Carl von Ossietzky University, Oldenburg, Germany*

²*Department of Physics, University of California, Santa Cruz, California 95064, USA*

(Dated: April 9, 2015)

We investigate numerically the time dependence of “window” overlaps in a three-dimensional Ising spin glass below its transition temperature after a rapid quench. Using an efficient GPU implementation, we are able to study large systems up to lateral length $L = 128$ and up to long times of $t = 10^8$ sweeps. We find that the data scales according to the ratio of the window size W to the non-equilibrium coherence length $\xi(t)$. We also show a substantial change in behavior if the system is run for long enough that it globally equilibrates, i.e. $\xi(t) \approx L/2$, where L is the lattice size. This indicates that the local behavior of a spin glass depends on the spin configurations (and presumably also the bonds) far away. We compare with similar simulations for the Ising ferromagnet. Based on these results, we speculate on a connection between the non-equilibrium dynamics discussed here and averages computed theoretically using the “metastate”.

PACS numbers: 75.50.Lk, 75.40.Mg, 75.10.Nr

I. INTRODUCTION

Spin glasses [1–3] below their transition temperature are not in equilibrium, except for very small sizes in some simulations. One therefore needs to be able to describe non-equilibrium behavior, and a lot of attention numerically [4–9] has been focussed on the evolution of the system after a rapid quench to temperature T below the transition temperature T_c . Locally, spins establish correlations so one anticipates that they will be correlated up to some distance, the coherence length $\xi(t)$, which slowly increases with time. For distances longer than $\xi(t)$ correlations will decay exponentially, while at shorter distances they will decay more slowly than that. Empirically one finds [4–9] that the growth of $\xi(t)$ is compatible with a small power of t (although a logarithmic growth cannot be fully excluded using the available data), written as $\xi(t) \sim t^{1/z(T)}$ where, $z(T)$, a non-equilibrium dynamic exponent is found to depend on the ratio T/T_c .

To understand the nature of the spin glass state one needs local probes, see e.g. [10] and references therein. A useful local probe is the distribution of the overlap q of the spins in two copies of the system in a window of linear size W . Equilibrium properties of window overlaps have been studied numerically before [11], but here we focus on their non-equilibrium behavior, which has not received much attention before apart from Ref. [6] which studied the non-equilibrium evolution of a dimensionless ratio of cumulant averages evaluated in windows of different size. In this paper we study the time dependence of the window overlap distribution $P_W(q)$, in a non-equilibrium situation. We find that the distribution scales as a function of the ratio of the window size W to $\xi(t)$. The non-equilibrium window overlap distribution is very different from the global equilibrium overlap distribution $P(q)$ in the mean field theory of Parisi [12–14]. In particular $P_W(0)$ depends quite strongly on W . However, if the system is run for a time long enough for the system to globally equilibrate, i.e. $\xi(t) \simeq L/2$, then

we find a change in the form of $P_W(q)$, which happens rapidly when viewed on a logarithmic time scale, such that $P(0)$ then has a rather a weak dependence on W and is quite similar to the $q = 0$ value of Parisi’s global equilibrium overlap distribution [14] $P(q)$. The strong change in behavior when $\xi(t) \simeq L/2$ indicates that local spin correlations are sensitive to spin orientations, and presumably also to the values of the interactions, at large (or at least intermediate) distances.

The theoretical description of spin glasses below T_c is complicated. One approach developed in recent years is known as the “metastate” [15–17]. In this paper we also speculate on a possible connection between non-equilibrium correlations following a quench, and averages computed according to the metastate.

The plan of this paper is as follows. In Sec. II we describe the metastate and a possible connection between quantities calculated from it and non-equilibrium averages following a quench. The model we simulate and the quantities we calculate are described in Sec. III. The results of the simulations are given in Sec. IV, together with corresponding results for a pure Ising ferromagnet, and our conclusions summarized in Sec. V.

II. AVERAGING IN SPIN GLASSES; THE METASTATE AND DYNAMICS

In systems undergoing phase transitions it is desirable to know what are the various possible states to which the system can evolve below the transition temperature T_c . A simple example is the Ising ferromagnet in zero magnetic field for which there is just a pair of states below T_c , related by flipping all the spins, the “up” and “down” spin states. If the system is in one of these states then “connected” correlation functions vanish at large distances, e.g.

$$\lim_{|\mathbf{R}_i - \mathbf{R}_j| \rightarrow \infty} [\langle S_i S_j \rangle - \langle S_i \rangle \langle S_j \rangle] = 0, \quad (1)$$

which is known as “clustering” of the correlation functions. The angular brackets $\langle \dots \rangle$ denote a thermal average, here restricted to one of these states to capture the symmetry breaking. By contrast if we simply perform the Boltzmann sum we give equal weight to both of these states, the symmetry is not broken so $\langle S_i \rangle = \langle S_j \rangle = 0$, and hence the two terms in Eq. (1) do not cancel at large distances and the correlation functions do not have a clustering property. States which do not have a clustering property are called “mixed” states and those that do, like the “up” and “down” states of the ferromagnet, are called “pure” states.

To keep the description of the system as simple as possible it is desirable to use clustering (i.e. pure) states. In many cases this is easy because they are just the different states in which a global symmetry of the Hamiltonian is broken. However, in more complicated situations such as spin glasses, there can be pure states not related by any symmetry and so characterizing them can be quite difficult. Nonetheless, it is argued [10, 15, 16, 18–23] to be important to describe spin glasses in terms of pure states rather than by computing the Boltzmann sum. The latter is done, for example, in the Parisi [12–14] solution of the infinite-range Sherrington-Kirkpatrick (SK) [24] model.

To define pure states in general, consider the situation in Fig. 1. The overall system is of very large size L and has free or periodic boundary conditions. We compute the thermal average exactly, and determine the correlation functions in a much smaller window of size W , somewhere in the bulk of the system. These correlations may have the clustering property, in which case the window is in a pure state, or they may not in which case it is in a mixed state. In fact, since we consider only zero field, states come in symmetry-related pairs, so the simplest situation would be a single pair of pure states.

But for a system like a spin glass, the correlations in the window could depend sensitively on the choice of interactions in distant regions of the of the system, perhaps even in a chaotic manner, an aspect first pointed out explicitly by Newman and Stein (NS) [22]. To investigate this we divide the system of size L into an inner region of size M , larger than the window of size W which is in the middle of it, and an outer region between L and M . We then change the bonds in the outer region and recompute the correlation functions in the window. Eventually we let all sizes tend to infinity with $L \gg M \gg W \gg 1$. It is possible that the state of the window is always the same as one changes the bonds in the outer region. However, it is also possible that the state changes, perhaps chaotically, as one changes the bonds in the outer region. Several possible situations have been discussed in detail:

- For each set of bonds in the outer region one has only a single pair of pure states, and one finds the *same* pair for every set of outer bonds. This is called the “droplet model” the theory for which has been developed in the greatest detail by Fisher and Huse [18–21].

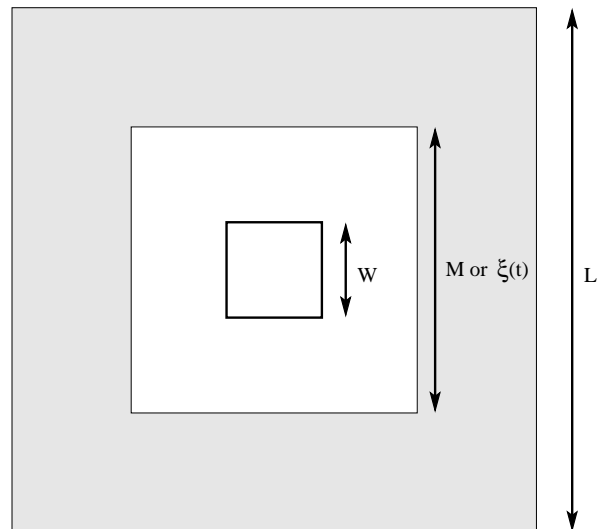


FIG. 1. The length scales that are needed to discuss the Aizenman-Wehr (AW) metastate. The overall size of the system is L , which is assumed to be very large and has periodic or free boundary conditions. We consider an outer region, of size between M and L , shown shaded, where we average over different bond configurations, and an inner region, unshaded, where we consider just a single set of bonds. Spin correlations will be studied in a window of size W , less than M . In the metastate, we require that the different length all ultimately tend to infinity such that $L \gg M \gg W \gg 1$. In our simulations, the length scales are, of course, finite (actually quite small) but we shall still view the situation in the simulations as analogous to the theoretical discussion, in which, as for the metastate, L is the size of the system (with periodic boundary conditions) and W is a small region where we measure correlations, but now M , the intermediate scale, is the *non-equilibrium coherence length* $\xi(t)$, the scale to which correlations have developed after a quench at time $t = 0$. In the simulations we can run for long enough, and take sufficiently small window sizes, to get data in the region where $\xi(t) > W$ as shown.

- For each set of bonds in the outer region one has only a single pair of pure states, but this pair varies chaotically as one changes the outer bonds. This is the “chaotic pairs” picture of NS [22].
- For each set of bonds in the outer region one has a mixed state, and this mixes changes in a chaotic way as the outer bonds are changed. This is called the “replica symmetry breaking” (RSB) picture¹ since it is the generalization to finite-range

¹ NS [15, 16] call this the “non-standard” RSB picture, because they showed that a different, “standard”, RSB picture is not viable. As also emphasized recently by Read [23], the “non-standard” picture is the only viable RSB picture, so we shall omit the term “non-standard” and just refer to this scenario as the “RSB picture”. In fact, Read also shows that the RSB calculations lead *directly* to the “non-standard” picture.

models of Parisi's [12–14] solution of the infinite-range SK model. The name arises because Parisi's original solution used the replica method to average over the disorder.

In order to describe the states of a spin glass one needs to give a *statistical* description of the different states the window can be in as the bonds in the outer region are varied. NS [15, 16] call this the metastate. The description that we give here is actually a little different from that of NS and is due to Aizenman and Wehr (AW) [17]. In NS's approach there is no intermediate scale M and one looks at the correlations in the window as the system size L is grown leaving the bonds already present unchanged. It is expected [25] that the two forms of the metastate are equivalent. In agreement with Read [23] we find that it is easier to discuss the AW metastate.

The AW metastate average is therefore performed by first doing a thermal average for the whole system, denoted by $\langle \cdots \rangle$, followed by an average over the bonds in the outer region, denoted by $[\cdots]_{\text{out}}$. Following Read [23] we call this the metastate-averaged state (MAS). Hence, if i and j lie within the window, the spin glass correlation function of their spins in the MAS is given by

$$C_{ij} = [\langle S_i S_j \rangle]_{\text{out}}^2, \quad (2)$$

(note the location of the square). After this average is done one can also average over the bonds in the inner region, which we denote by $[\cdots]_{\text{in}}$. We will present data for the window overlap distribution for which averaging over the bonds in the inner region is, strictly, speaking, unnecessary since translation invariant MAS averages are self-averaging [15, 16, 26]. However, in practice, this last average *is* done in simulations to improve statistics.

It is interesting to ask how the MAS average C_{ij} varies at large distance R_{ij} ($\equiv |\mathbf{R}_i - \mathbf{R}_j|$) according to the three scenarios mentioned above:

- In the droplet picture one finds always the same pair of thermodynamic states so presumably

$$\lim_{R_{ij} \rightarrow \infty} C_{ij} = q^2, \quad (3)$$

where $q = \langle S_i \rangle^2$ is the Edwards-Anderson order parameter, which is well defined if we add a small symmetry-breaking field to remove the degeneracy between the pair of pure states. Equation (3) then follows because of clustering of correlations in a single pure state, see Eq. (1). We should mention, though, that the approach to the constant value of q^2 is expected to be quite slow, a power-law rather than an exponential, and so, for the values of R_{ij} that one can simulate, one may be far from the constant value (David Huse, private communication).

- In the chaotic pairs picture, correlations in the window alter, in sign as well as magnitude, as the outer bonds are varied. Hence, according to Read [23], it

is expected that C_{ij} tends to zero, presumably as a power law, which is commonly written as

$$C_{ij} \propto \frac{1}{R_{ij}^{d-\zeta}}, \quad (4)$$

for $R_{ij} \rightarrow \infty$, which defines the exponent ζ .

- In the RSB picture, which also has many states, MAS averaged correlations are similarly expected to decay as the power law in Eq. (4). In fact ζ has been calculated in mean field theory [23, 27–29] (corresponding to $d > 6$) assuming RSB, with the result $\zeta = 4$.

A large spin glass system is not in thermal equilibrium below T_c . Results from the Boltzmann sum do not, therefore, correspond to experimental observations which are inevitably in a non-equilibrium situation. Are MAS averages any better in this regard? It is tempting to think so for the following reason.

Imagine quenching the spin glass to below T_c and observing correlations in a local window of size W . Correlations will develop up to some coherence length $\xi(t)$ which grows slowly with time. How does one expect the non-equilibrium correlation function

$$C_t(i, j) = [\langle S_i(t) S_j(t) \rangle]^2, \quad (5)$$

where $[\cdots]$ denotes an average over *all* the bonds, to vary as a function of R_{ij} ? Let us assume that time is large enough that $\xi(t) > W$. We postulate that thermal fluctuations of the spins outside the window at a distance $\xi(t)$ and greater, which are not equilibrated with respect to spins in the window, effectively generate a random noise to the spins in the window which plays a similar role to the random perturbation coming from changing the bonds in the outer region according to the AW metastate, see Fig. 1. Thus we suggest that $\xi(t)$ is analogous to the intermediate scale M , separating inside and outside regions, in the construction of the metastate. This is indicated in Fig 1. After this work was submitted it was brought to our attention that a similar picture of non-equilibrium dynamics following a quench was discussed earlier by White and Fisher [30]. They denote the state obtained after a quench as the “maturation metastate” and the distribution of states in the AW or NS picture as the “equilibrium metastate”. Here we speculate that these might be the same. We thank Nick Read for bringing this paper to our attention.

This analogy suggests that the decay of correlations determined from the metastate may be the same as the decay of correlations following a quench, on scales shorter than the coherence length. We note that NS have also discussed dynamics following a quench [31, 32] from a rigorous point of view.

There have been many simulations which investigate the time dependence of correlations following a quench [4–9]. Interestingly these papers *do* see a power

L	N_{samp}	
	Spin glass	Ferromagnet
128	192	64
64	-	512
32	-	512
20	512	-
16	768	2048
12	1024	-

TABLE I. The number of samples studied for different system sizes.

law decay of the correlation function in Eq. (5) for sufficiently long times that $\xi(t) > R_{ij}$, i.e.

$$C_t(i, j) \propto \frac{1}{R_{ij}^\alpha} \quad \text{for} \quad R_{ij} \ll \xi(t) \ll L. \quad (6)$$

The exponent α is found to be about 1/2 in three dimensions [4–9]. Equation (6) is of the same form as Eq. (4) which is obtained from metastate calculations for the Edwards-Anderson model [23, 29] in the mean field approximation, assuming the RSB picture. The droplet theory predicts a different result, namely Eq. (3), though, of course, the numerical data may not be at large enough length scales to be in the asymptotic scaling regime.

III. THE MODEL AND QUANTITIES TO BE CALCULATED

We simulate the Edwards-Anderson [33] Ising spin glass model with Hamiltonian

$$\mathcal{H} = - \sum_{\langle i, j \rangle} J_{ij} S_i S_j, \quad (7)$$

where the spins S_i take values ± 1 and are on the sites of a simple cubic lattice with $N = L^3$ spins with periodic boundary conditions. The quenched interactions J_{ij} are between nearest neighbors and take values ± 1 with equal probability. The latest determination of the transition temperature of this model is $T_c = 1.102(3)$ [34]. Here we work at a fixed temperature of $T = 0.8 \simeq 0.73T_c$. Most of the simulations are for system size $L = 128$, which can not be brought to equilibrium in available computer time, but we also perform some simulations at smaller sizes to investigate the change in behavior when the system reaches global equilibrium. The number of samples simulated for each size is shown in Table I.

We run two copies of the system with the same bonds but different initial random spin configurations, which we quench to $T = 0.8$ at time $t = 0$, and then let the system evolve. To perform long runs on large lattices we have implemented an efficient Monte Carlo code on GPUs, see [9] for details. At a logarithmically increasing set of times we store the spin configurations from which we calculate the correlation function in Eq. (5) as a function of R_{ij} at different times.

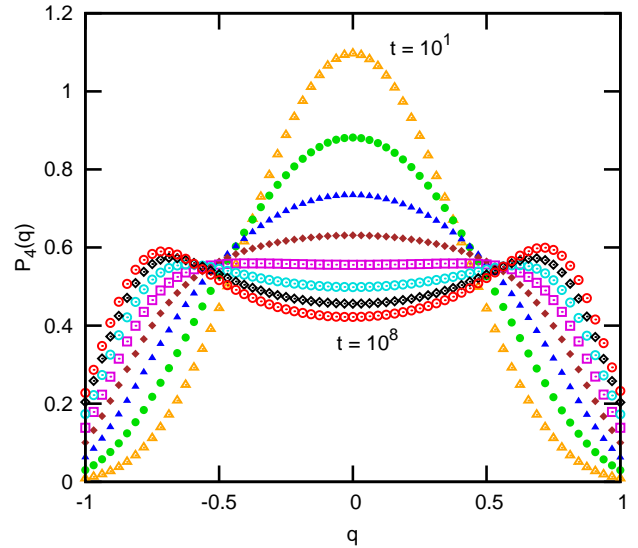


FIG. 2. (Color online) A representative set of results for the window overlap distribution, for window size $W = 4$ for lattice size $L = 128$ at $T = 0.8$. Data is shown for times $t = 10^k$, where $k = 1, 2, \dots, 8$.

We also compute the time-dependent window overlap distribution defined by

$$P_W(q) = [\langle \delta(q - q^{1,2}) \rangle], \quad (8)$$

where $q^{1,2}$, the window overlap between replicas “(1)” and “(2)”, is

$$q^{1,2} = \frac{1}{W^d} \sum_{i=1}^{W^d} S_i^{(1)} S_i^{(2)}, \quad (9)$$

in which the sum is over the sites in the window and, for ease of notation, we have suppressed an index t on $P_W(q)$ which would indicate that it also depends on time. To improve statistics we average over all non-overlapping windows of size W . The number of these is $\lfloor L/W \rfloor^d$ where $\lfloor \dots \rfloor$ indicates rounding down to the nearest integer. In addition, we smooth the data by computing, for each discrete value of the overlap, q_0 say, an average of the distribution on neighboring q -values weighted by a normalized kernel which falls to zero as $|q - q_0|$ increases [35].

IV. RESULTS

A. Spin Glass

An example of our data for the window overlap distribution is shown in Fig. 2 for $W = 4$. One sees an evolution from a single peak structure at short times, presumably Gaussian, to a two-peaked structure at long times. For larger window sizes, the distribution evolves

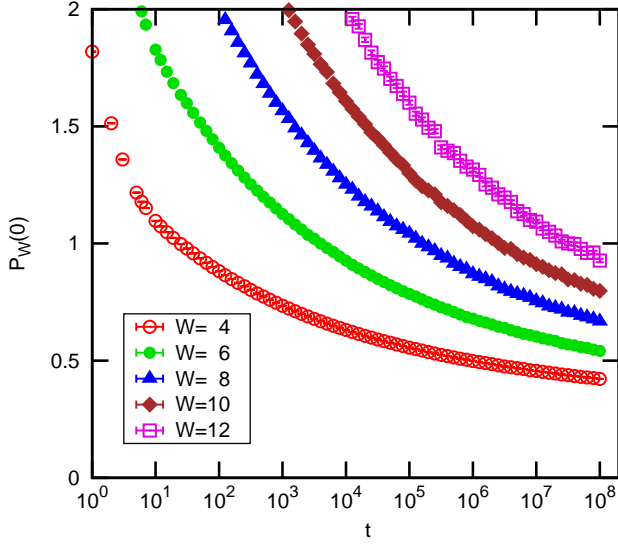


FIG. 3. (Color online) Results for the weight in the window overlap distribution at $q = 0$ for different window sizes as a function of time. The lattice size is $L = 128$ and $T = 0.8$.

more slowly, as shown in the data for $P_W(0)$, the weight of the distribution at $q = 0$, for different sizes in Fig. 3.

We would like to perform a scaling collapse of the data in Fig. 3 to ascertain the dependence of $P_W(0)$ on t and W . However, rather than scaling with respect to t we find it better to scale with the dynamic coherence length $\xi(t)$. At long times, where $\xi(t) \gg R_{ij}$, the time-dependent correlation function in Eq. (5) varies with an inverse power of R_{ij} as shown in Eq. (6), so a natural scaling ansatz is

$$C_t(i, j) = \frac{1}{R_{ij}^\alpha} g\left(\frac{R_{ij}}{\xi(t)}\right). \quad (10)$$

The coherence length $\xi(t)$ can be taken from a ratio of moments of $C_t(i, j)$ [8], e.g.

$$\xi(t) = \frac{\int_0^{L/2} r^2 C_t(r) dr}{\int_0^{L/2} r C_t(r) dr}. \quad (11)$$

In practice the integral is performed along x, y and z axes. The data for $\xi(t)$ obtained in this way in Ref. [9] is shown in the inset to Fig. 4.

Note that this calculation of $\xi(t)$ did not make any reference to a window. However, if we compute the second moment of the window overlap distribution, $[\langle q^2 \rangle]$, we note first that it is just the average of $C_t(i, j)$ over all

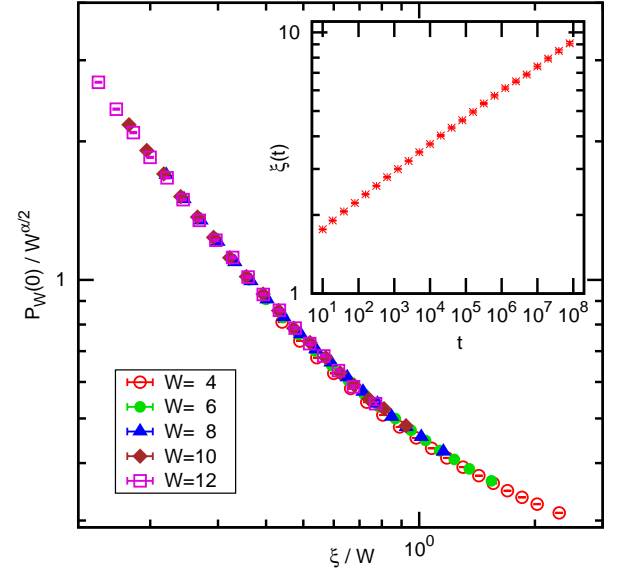


FIG. 4. (Color online) The main figure shows a scaling plot of $P_W(0)/W^{\alpha/2}$ against ξ/W , in which we used the results for $\xi(t)$ shown in the inset, which are obtained in Ref. [9], and took the value $\alpha = 0.438$ also from Ref. [9]. The data collapse is excellent. The data is for system size $L = 128$ and $T = 0.8$.

sites i and j in the window since

$$\begin{aligned} [\langle q^2 \rangle] &= \frac{1}{W^6} \sum_{i,j} \left[\langle S_i^{(1)} S_i^{(2)} S_j^{(1)} S_j^{(2)} \rangle \right] \\ &= \frac{1}{W^6} \sum_{i,j} \left[\langle S_i^{(1)} S_j^{(1)} \rangle \langle S_i^{(2)} S_j^{(2)} \rangle \right] \\ &= \frac{1}{W^6} \sum_{i,j} C_t(i, j). \end{aligned} \quad (12)$$

Using Eq. (10) this can be written as

$$\begin{aligned} [\langle q^2 \rangle] &= \frac{1}{W^6} \int_{R,R'} dR dR' |R - R'|^{-\alpha} g(|R - R'|/\xi) \\ &\sim \frac{1}{W^6} \int_R \int_0^{W/2} dr 4\pi r^2 r^{-\alpha} g(r/\xi) \\ &= W^{-\alpha} 4\pi \int_0^{1/2} dx x^{2-\alpha} g(xW/\xi) \\ &= W^{-\alpha} f\left(\frac{W}{\xi}\right), \end{aligned} \quad (13)$$

where we used the substitution $x = r/W$ in the next to last line.

If we divide q by an arbitrary scale factor λ the distribution of $q' (= q/\lambda)$ is $\bar{P}(q')$ where $P(q) = \lambda^{-1} \bar{P}(q/\lambda)$ because both distributions are normalized. If we take $\lambda = \sigma$, the standard deviation of $P(q)$, then $P(0) = \sigma^{-1} \bar{P}(0)$. But $\bar{P}(q')$ has standard deviation unity, and so, if the distribution is smooth and extends down to the origin,

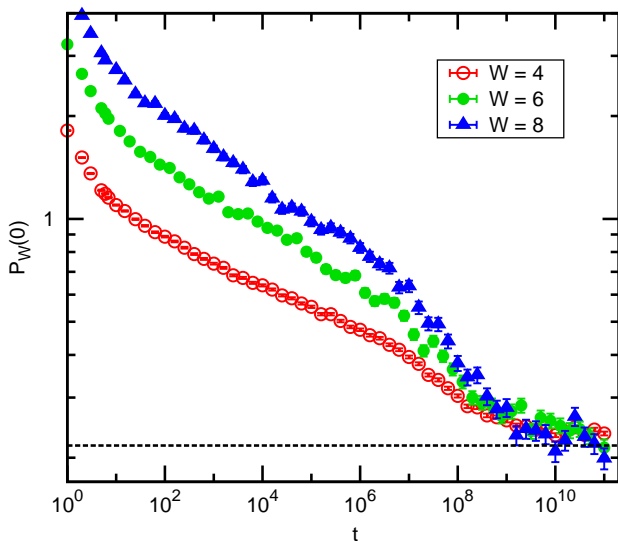


FIG. 5. (Color online) Data for $P_W(0)$ for different values of W for size $L = 16$. At time in the range 10^7 – 10^9 this rather small system fully equilibrates leading to a decrease in the data which is quite rapid on this log scale. The dashed line shows the equilibrium value of the *bulk* order parameter distribution for $L = 16$, i.e. $W = L = 16$. One sees that the *equilibrium* values of $P_W(0)$ for $W < L$ are very similar to that of the bulk overlap.

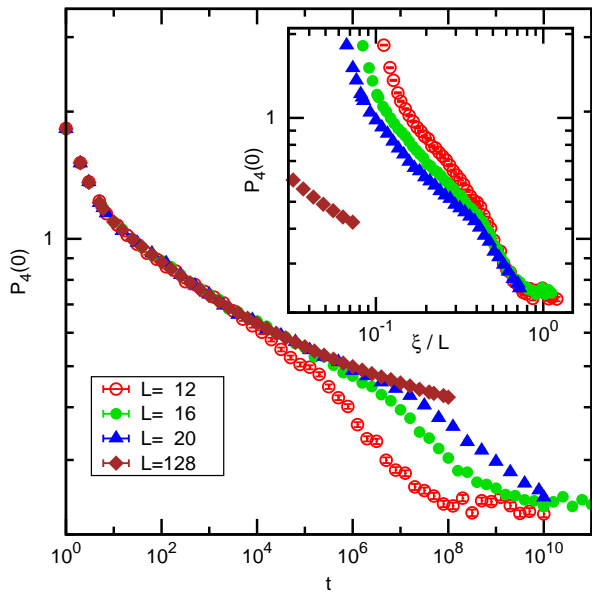


FIG. 6. (Color online) Data for $P_4(0)$ for different system sizes at $T = 0.8$. For the three smaller sizes, $L = 12, 16$ and 20 the system equilibrates, leading to a pronounced drop in the data, at a time which increases with L . The inset plots the same data against ξ/L where for ξ we use a fit to the data in the inset of Fig. 4. The collapse of the data in the region where it decreases, which is quite rapid on this log scale, shows that the decrease occurs when ξ is a fixed fraction (about $1/2$) of the system size, indicating full equilibration.

we have $\overline{P}(0) \sim 1$ and hence $P(0) \sim \sigma^{-1}$. Consequently, from Eq. (13), the expected scaling of $P_W(0)$ is

$$P_W(0) = W^{\alpha/2} F\left(\frac{\xi}{W}\right). \quad (14)$$

For t large but still smaller than the time to equilibrate the whole system, the dependence on ξ must drop out and so

$$P_W(0) \propto W^{\alpha/2} \quad \text{for } W \ll \xi(t) \ll L. \quad (15)$$

For short times where $\xi(t) \ll W$ the spins in the window are random, so the mean square window overlap goes like $1/W^d$ (in d dimensions) and consequently $P_W(0) \propto W^{d/2}$. Presumably we then have $F(x) \propto x^{-(d-\alpha)/2}$ for $x \rightarrow 0$. This actually gives $P_W(0) \propto W^{d/2}/\xi^{(d-\alpha)/2}$ but when $\xi(t) \lesssim 1$ corrections to scaling occur which cause ξ to be replaced by a cutoff of order unity and so one obtains the desired result.

We take $\xi(t)$ from Ref. [9], evaluated according to Eq. (11), and also use the value of α from Ref. [9], $\alpha = 0.438(11)$. This exponent has also been computed in Ref. [8] with a very similar value, $\alpha = 0.442(11)$. The result of scaling the data in Fig. 3 according to Eq. (14) is shown in the main part of Fig. 4. Clearly the scaling collapse works very well.

The power law decay of correlation in Eq. (6), and the resulting behavior of the window order parameter distribution in Eq. (14), are for a non-equilibrium situation where $\xi(t) \ll L$. However, we shall now see that a dramatic change occurs at sufficiently long times that global equilibrium occurs, i.e. when $\xi(t) \sim L/2$. In this region, we will find that the correlation function no longer decays to zero because there is spin glass order in equilibrium, and the weight of the window distribution at $q = 0$ [11, 29] becomes roughly independent of window size rather than increasing with window size in the manner shown in Eq. (14).

We demonstrate this change in behavior for the window overlaps explicitly as a function of time in Figs. 5 and 6. Since equilibrating size $L = 128$ is completely infeasible we show data for smaller sizes which we *can* bring to global equilibrium. Figure 5 shows results for $L = 16$ with window sizes $W = 4, 6$ and 8 . A rapid decrease is seen for t in the region 10^7 – 10^9 to a value which is independent of window size. As will be confirmed in Fig. 6, the data after the drop represents global equilibrium. The dashed line in Fig. 5 is the *bulk* value of the equilibrium overlap distribution at $q = 0$ and we see that this value is very similar to that of equilibrium *window* overlaps, as was also found earlier [11, 29].

To confirm that this change in behavior occurs when $\xi \sim L/2$ we plot results for $P_W(0)$ for a fixed window size but different system sizes in Fig. 6. For short times the data is independent of L indicating that $\xi \ll L$, but at later times a more rapid decrease occurs at a time which increases with L . The inset shows the data plotted against ξ/L clearly demonstrating that the region

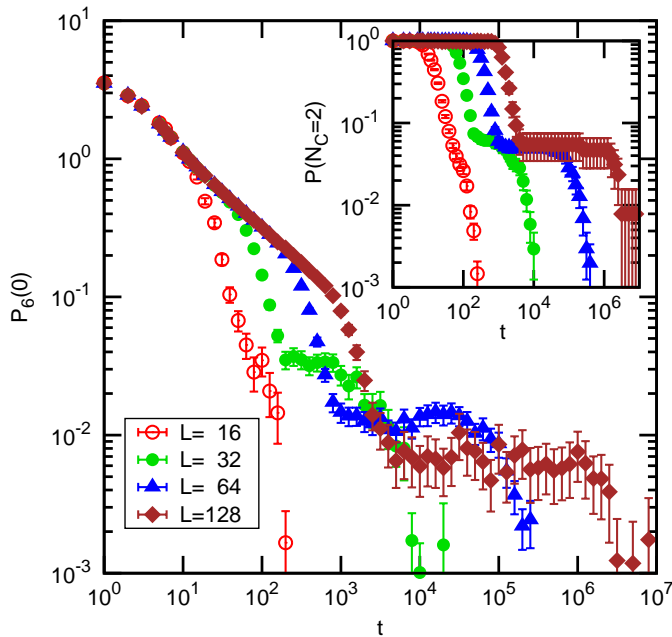


FIG. 7. (Color online) Data for $P_6(0)$ for different system sizes at $T = 3.6 \simeq 0.80T_c$ for the ferromagnet. The plateau at intermediate times becomes longer for larger L . The explanation is that a fraction of the runs gets stuck in a state with two big domains for a long time, thus contributing a certain number of overlaps with $q \simeq 0$. The inset shows the probability that two large domains coexist.

with rapid decrease occurs when ξ/L is about $1/2$. This confirms that the decrease is associated with complete equilibration of the system.

B. Ferromagnet

For comparison we also did simulations of the ferromagnet, $p = 1.0$, at temperature $T = 3.6$. Since $T_c \simeq 4.51$ for the ferromagnet, this corresponds to $T = 0.80T_c$, a similar fraction of T_c as used in the spin glass simulations. The number of samples is detailed in Table I. It should be pointed out that we are still using a single random number for multiple samples (due to multi-spin coding techniques) but with different initial configurations, as is common practice for spin-glass simulations. But in ferromagnetic equilibrium this causes the samples to become almost completely correlated. However, before equilibration, due to the different initial configurations, the dynamics of the different samples is different.

Data for the window overlap for window size $W = 6$ and different lattice sizes are shown in Fig. 7. Even our largest systems can be equilibrated, as indicated by the data dropping to a very small value ($< 10^{-3}$) at the longest times. Note that the value of $P_W(0)$ is not exactly zero even when the system has fully equilibrated because of rare thermal fluctuations. At short times the decay is

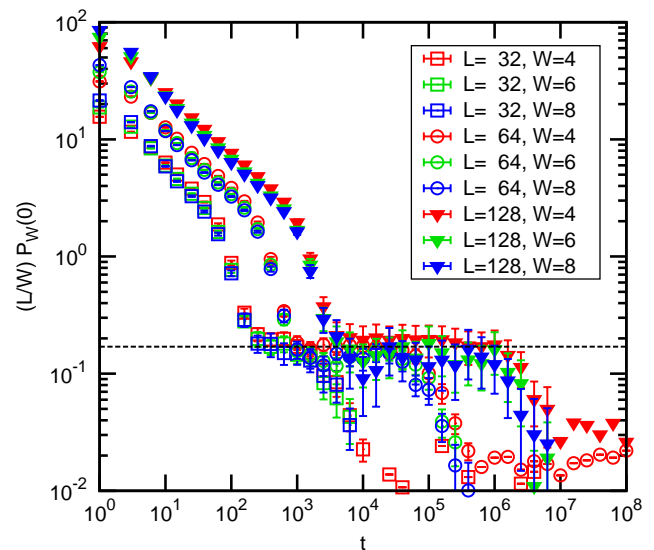


FIG. 8. (Color online) Plot of $P_W(0)$ multiplied by the ratio of the system size L to the window size W for different values of W and L at $T = 3.6 \simeq 0.80T_c$ for the ferromagnet. On this plot the height of the plateau at intermediate times seems to be independent of L and W showing that $P_W(0)$ itself is proportional to W/L , which we interpret as the probability that a straight domain wall goes through the window. The dashed horizontal line is a guide to the eye.

roughly $t^{-1/2}$ as expected from coarsening [36], according to which $\xi(t)$, the typical domain size, grows proportional to $t^{1/2}$. However, in addition, a plateau appears at intermediate times. We shall see that this plateau occurs because in some runs, even when the correlation length has grown to the size of the system, a single domain with straight walls persists for a much longer time. Evidence for this is shown in the inset to Fig. 7 which plots the probability of finding two large clusters of oppositely oriented spins. This quantity has plateaus for the same range of time as the data for $P_6(0)$ shown in the main part of the figure.

Figure 8 plots data for different system sizes and window sizes, and shows that the *height* of the plateau is proportional to W/L which has a straightforward interpretation as the probability that a straight domain wall passes through the window.

We find that the *time* at the *beginning* of the plateau varies as L^2 , which is expected since it is the time for the coherence length to grow to the system size according to the coarsening picture in which $\xi(t) \propto t^{1/2}$. The time at the *end* of the plateau grows more rapidly and we find empirically it is roughly proportional to $L^{4.8}$. We presume that this is the time scale needed for a random walk of the (straight) domain walls to cause the domains to meet and form one big domain. S. Redner (private communication) has argued that this exponent is exactly four, and our data is consistent with this value.

The rich dynamics of three-dimensional Ising ferro-

magnets after a quench have been studied in great detail, see e.g. [37], at very low and zero temperature. By contrast, our results are for a much higher temperature, though still below T_c . Based on the preliminary findings presented here, we feel it would be interesting to study this region in more detail in the future.

V. CONCLUSIONS

We have shown that the non-equilibrium window overlap distribution of a spin glass following a quench to below T_c can be well characterized by the ratio of the dynamic coherence length $\xi(t)$ to the window size W . For a fixed W the distribution tends to a well defined limit at long times such that $\xi(t) \gg W$ but where $\xi(t)$ is still much less than the system size L . This distribution depends strongly on W ; for example $P_W(0) \propto W^{\alpha/2}$ where $\alpha \simeq 0.44$.

However, if we can run the simulation for sufficiently long times that the system globally equilibrates, i.e. $\xi(t) \simeq L/2$, then there is a change in behavior, which is abrupt when plotted on a logarithmic time scale, see Fig. 6, such that $P_W(0)$ then only depends weakly on W and is very similar to the value at zero overlap of Parisi's global overlap distribution $P(q)$. Though a similar looking plateau was found for the not-quite fully equilibrated ferromagnet, characterized by the existence of domain walls, it was qualitatively different since the height of the plateau depends on the overall system size L for the ferromagnet. By contrast, for the spin glass, the data in Fig. 6, while admittedly not *fully* in the plateau re-

gion, does not show any dependence on L until the final equilibrium is reached (the *end* of the plateau).

The strong change in behavior for the spin glass when $\xi(t) \simeq L/2$ indicates that local spin correlations are sensitive to spin orientations, and presumably also to the values of the interactions, at large distances. According to the droplet theory, the local state of the system does *not* depend on the values of the interactions sufficiently far away. If the droplet theory is correct asymptotically, the length-scale beyond which this independence occurs must be much larger than the system sizes we have been able to equilibrate below T_c (namely $L = 16$).

In addition, we have speculated on a possible connection between the non-equilibrium dynamics discussed here and averages computed theoretically using the “metastate”. For a future better understanding of this possible connection via numerical simulations a more intense use of powerful yet rather cheap devices as GPUs, like in the present work [9], or the application of new algorithms like population annealing to spin glasses [38, 39] might be useful.

ACKNOWLEDGMENTS

MM and AKH thank Martin Weigel for interesting discussions. We would like to thank Nick Read and David Huse for a most informative correspondence, and Sid Redner for suggesting the exact value of the exponent giving the length of the plateau in Fig. 8. The work of APY is supported in part by the National Science Foundation under Grant No. DMR-1207036, and by a Research Award from the Alexander von Humboldt Foundation.

-
- [1] K. Binder and A. P. Young, *Spin glasses: Experimental facts, theoretical concepts and open questions*, Rev. Mod. Phys. **58**, 801 (1986).
 - [2] M. Mézard, G. Parisi, and M. A. Virasoro, *Spin Glass Theory and Beyond* (World-Scientific, 1987).
 - [3] A. P. Young, ed., *Spin Glasses and Random Fields* (World Scientific, Singapore, 1998).
 - [4] H. Rieger, *Non-equilibrium dynamics and aging in the three-dimensional Ising spin-glass model*, J. Phys. A **26**, L615 (1993).
 - [5] J. Kisker, L. Santen, M. Schreckenberg, and H. Rieger, *Off-equilibrium dynamics in finite-dimensional spin-glass models*, Phys. Rev. B **53**, 6418 (1996).
 - [6] E. Marinari, G. Parisi, F. Ritort, and J. J. Ruiz-Lorenzo, *Numerical evidence for spontaneously broken replica symmetry in 3d spin glasses*, Phys. Rev. Lett. **76**, 843 (1996).
 - [7] H. Yoshino, K. Hukushima, and H. Takayama, *Extended droplet theory for aging in short-range spin glasses and a numerical examination*, Phys. Rev. B **66**, 064431 (2002).
 - [8] F. Belletti et al, *An in-depth view of the microscopic dynamics of Ising spin glasses at fixed temperature*, J. Stat. Phys. **135**, 1121 (2009), (arXiv:0811.2864).
 - [9] M. Manssen and A. K. Hartmann, *Ageing at the Spin Glass/Ferromagnet Transition: Monte Carlo Simulation using GPUs* (2014), preprint arXiv:1411.5512.
 - [10] C. Newman and D. L. Stein, *Ordering and broken symmetry in short-ranged spin glasses*, J. Phys.: Cond-Mat **15**, R1319 (2003).
 - [11] E. Marinari, G. Parisi, F. Ricci-Tersenghi, and J. J. Ruiz-Lorenzo, *Small window overlaps are effective probes of replica symmetry breaking in three-dimensional spin glasses*, J. Phys. A **31**, L481 (1998).
 - [12] G. Parisi, *Infinite number of order parameters for spin-glasses*, Phys. Rev. Lett. **43**, 1754 (1979).
 - [13] G. Parisi, *The order parameter for spin glasses: a function on the interval 0–1*, J. Phys. A. **13**, 1101 (1980).
 - [14] G. Parisi, *Order parameter for spin-glasses*, Phys. Rev. Lett. **50**, 1946 (1983).
 - [15] C. Newman and D. L. Stein, *Spatial inhomogeneity and thermodynamic chaos*, Phys. Rev. Lett. **76**, 4821 (1996).
 - [16] C. Newman and D. L. Stein, *Metastate approach to thermodynamic chaos*, Phys. Rev. E **55**, 5194 (1997).
 - [17] M. Aizenman and J. Wehr, *Rounding effects of quenched randomness on first-order phase transitions*, Comm. Math. Phys. **130**, 489 (1990).
 - [18] D. S. Fisher and D. A. Huse, *Ordered phase of short-range Ising spin-glasses*, Phys. Rev. Lett. **56**, 1601 (1986).
 - [19] D. S. Fisher and D. A. Huse, *Pure states in spin glasses*,

- J. Phys. A **20**, L997 (1987).
- [20] D. S. Fisher and D. A. Huse, *Absence of many states in realistic spin glasses*, J. Phys. A **20**, L1005 (1987).
 - [21] D. S. Fisher and D. A. Huse, *Equilibrium behavior of the spin-glass ordered phase*, Phys. Rev. B **38**, 386 (1988).
 - [22] C. Newman and D. L. Stein, *Multiple states and thermodynamic limits in short-ranged Ising spin-glass models*, Phys. Rev. B **46**, 973 (1992).
 - [23] N. Read, *Short-range Ising spin glasses: the metastate interpretation of replica symmetry breaking*, Phys. Rev. E **90**, 032142 (2014), (arXiv:1407.4136).
 - [24] D. Sherrington and S. Kirkpatrick, *Solvable model of a spin glass*, Phys. Rev. Lett. **35**, 1792 (1975).
 - [25] C. Newman and D. L. Stein, *Thermodynamic Chaos and the Structure of Short-Range Spin Glasses*, in *Mathematics of Spin Glasses and Neural Networks*, edited by A. Bovier and P. Picco (Birkhauser, Boston, 1997).
 - [26] C. Newman and D. L. Stein, *Non-mean-field behavior of realistic spin glasses*, Phys. Rev. Lett. **76**, 515 (1996).
 - [27] C. de Dominicis, I. Kondor, and T. Temesvári, in *Spin glasses and random fields*, edited by A. P. Young (World Scientific, Singapore, 1998), (arXiv:cond-mat/9705215).
 - [28] C. De Dominicis and I. Giardinà, *Random Fields and Spin Glasses* (Cambridge University, Cambridge, 2006).
 - [29] E. Marinari, G. Parisi, F. Ricci-Tersenghi, J. J. Riuz-Lorenzo, and F. Zuliani, *Replica symmetry breaking in short range spin glasses: A review of the theoretical foundations and of the numerical evidence*, J. Stat. Phys. **98**, 973 (2000), (arXiv:cond-mat/9906076).
 - [30] O. L. White and D. S. Fisher, *Scenario for spin-glass phase with infinitely many states*, Phys. Rev. Lett. **96**, 137204 (2006).
 - [31] C. M. Newman and D. L. Stein, *The Effect of Pure State Structure on Nonequilibrium Dynamics*, J. Phys.: Cond. Matt. **20**, 244132 (2008), (arXiv:0710:0633).
 - [32] C. Newman and D. L. Stein, *Equilibrium Pure States and Nonequilibrium Chaos*, J. Stat. Phys. **94**, 709 (1999).
 - [33] S. F. Edwards and P. W. Anderson, *Theory of spin glasses*, J. Phys. F **5**, 965 (1975).
 - [34] M. Baity-Jesi et al, *Critical parameters of the three-dimensional Ising spin glass*, Phys. Rev. B **88**, 224416 (2013), (arXiv:1310.2910).
 - [35] R. Alvarez Banos et al, *Nature of the spin-glass phase at experimental length scales*, J. Stat. Mech. p. P06026 (2010), (arXiv:1003.2569).
 - [36] A. J. Bray, *Theory of phase-ordering kinetics*, Adv. Phys. **51**, 481 (2002).
 - [37] J. Olejarz, P. Krapivsky, and S. Redner, *Zero-Temperature Relaxation of Three-Dimensional Ising Ferromagnets*, Phys. Rev. E **83**, 051104 (2011), (arXiv:1101.0762).
 - [38] J. Machta, *Population annealing with weighted averages: A monte carlo method for rough free-energy landscapes*, Phys. Rev. E **82**, 026704 (2010).
 - [39] W. Wang, J. Machta, and H. G. Katzgraber, *Evidence against a mean-field description of short-range spin glasses revealed through thermal boundary conditions*, Phys. Rev. B **90**, 184412 (2014).